HIV-1 Tat C modulates NOX2 and NOX4 expressions through miR-17 in a human microglial cell line

Jadhav, Vaishnavi Sunil; Krause, Karl-Heinz; Singh, Sunit K

ORIGINAL ARTICLE

HIV-1 Tat C modulates NOX2 and NOX4 expressions through miR-17 in a human microglial cell line

Vaishnavi Sunil Jadhav,* Karl-Heinz Krause† and Sunit K. Singh*,[1]

*Laboratory of Neurovirology and Inflammation Biology, CSIR-Centre for Cellular and Molecular Biology (CCMB), Hyderabad, India

†Department of Pathology and Immunology, Geneva Medical Faculty and University Hospitals, Centre Medical Universitaire, Geneva 4, Switzerland

Abstract

HIV-1 invades CNS in the early course of infection, which can lead to the cascade of neuroinflammation. NADPH oxidases (NOXs) are the major producers of reactive oxygen species (ROS), which play important roles during pathogenic insults. The molecular mechanism of ROS generation via microRNA-mediated pathway in human microglial cells in response to HIV-1 Tat protein has been demonstrated in this study. Over-expression and knockdown of microRNAs, luciferase reporter assay, and site-directed mutagenesis are main molecular techniques used in this study. A significant reduction in miR-17 levels and increased NOX2, NOX4 expression levels along with ROS production were observed in human microglial cells upon HIV-1 Tat C exposure. The validation of NOX2 and NOX4 as direct targets of miR-17 was done by luciferase reporter assay. The over-expression and knockdown of miR-17 in human microglial cells showed the direct role of miR-17 in regulation of NOX2, NOX4 expression and intracellular ROS generation. We demonstrated the regulatory role of cellular miR-17 in ROS generation through over-expression and knockdown of miR-17 in human microglial cells exposed to HIV-1 Tat C protein.

Keywords: CNS, HIV-1 Tat, microglia, microRNA, NADPH oxidases, ROS.

J. Neurochem. (2014) **131**, 803–815.

Human immunodeficiency virus (HIV) belongs to genus lentivirus and *Retroviridae* family, whose characteristic tendency is to cause subacute neurologic disease in host (Mayer and Schmidtmayerova 1997). Approximately 70% of HIV-infected patients develop HIV-associated neurological disorders during different stages of disease development (Clark and Vinters 1987). HIV enters in brain through infected monocytes/macrophages (Trojan horse mechanism) by compromising blood–brain barrier permeability during early course of acute infection (Koenig *et al.* 1986; Hazleton *et al.* 2010; Dohgu *et al.* 2011). Neurons are not directly infected by HIV, although other cells like astrocytes, microglia and perivascular macrophages get productively infected and serve as HIV reservoir. HIV has been isolated from CNS of AIDS patients with or without neuropsychiatric sequelae (Mayer and Schmidtmayerova 1997). HIV affects uninfected cells in a bystander fashion through the extracellularly secreted HIV proteins like Tat (Eugenin and Berman 2007; Li *et al.* 2009b). HIV-1 transactivator of transcription

(Tat) is a regulatory protein and among the early HIV proteins to be produced after infection. HIV Tat protein has been reported in serum of HIV-1-infected patients (Westendorp *et al.* 1995; Goldstein 1996; Xiao *et al.* 2000), where its concentration can reach up to 300–500 ng/mL (Poggi *et al.* 2004). HIV Tat protein is released from HIV-1-infected cells (Ensoli *et al.* 1990) and can be efficiently taken up by

ORIGINAL ARTICLE

neighboring cells, where it can alter the host gene expression including small RNAs in a bystander manner (Li *et al.* 2009b).

MicroRNAs are 19–23 nucleotides, non-coding, small RNAs which bind to complementary region, within 3′UTR (untranslated regions) of target genes through its seed region and regulate the expression of target genes (Lee *et al.* 2003; Bartel 2004; Singh 2007). HIV 1 Tat protein is extensively reported to modulate the expression of microRNAs (Eletto *et al.* 2008). We previously reported microRNA-mediated regulation of various genes (Mishra *et al.* 2012; Mishra and Singh 2013) in human microglial cells and brain microvascular endothelial cells in response to HIV-1 Tat C protein.

Microglial cells are brain resident macrophages, whose state of activation decides its role in protection or inflammation. Three phenotypic states of microglia are known; first, the ramified state, which is a resting state; second, the activated non-phagocytic state (found in areas involved in CNS inflammation), and third is the reactive, phagocytic state (found in areas of trauma or cell injury) (Frei *et al.* 1987; Suzumura *et al.* 1987; Williams *et al.* 1992; Panek and Benveniste 1995; Walker *et al.* 1995). Upon activation, microglial cells undergo morphological changes and alterations in patterns of gene expression profiles (Tambuyzer *et al.* 2009). Microglial cells have the ability to produce reactive oxygen species (ROS) through NADPH oxidases (NOX). Seven isoforms of NADPH oxidases (NOX1, NOX2, NOX3, NOX4, NOX5, DUOX1, and DUOX2) have been reported to play roles in ROS production. Out of these, NOX2 and NOX4 are well studied for their predominant role in ROS generation. NOX2 and NOX4 are known to be expressed in microglial cells (Lavigne *et al.* 2001; Vilhardt *et al.* 2002; Sorce and Krause 2009). Activation of NOX2 (also known as gp91^{phox}) takes place via interaction of various NOX subunits. Its interaction with p22^{phox} and association of cytosolic factors p47^{phox}, p67^{phox} to NOX2/p22^{phox} are required for its activation (Groemping and Rittinger 2005). NOX4 is p22^{phox}-dependent enzyme and does not need cytosolic subunits for its activation (Martyn *et al.* 2006). ROS is produced mostly by NOX enzymes in microglial cells (Babior 2004), as a defense mechanism. However, the excessive generation of ROS through NOX genes upon microglial activation could lead to neurotoxicity.

ROS results in elevated cytokine and chemokine production by microglial cells, thus indicating activation of microglial cells (Qin *et al.* 2004; Block and Hong 2005; Yang *et al.* 2007). Activated microglia are known to secrete various pro-inflammatory cytokines, which play important roles in neuroinflammation (Jovanovic 2012; Baby *et al.* 2014). ROS is known to aggravate HIV-associated diseases among AIDS patients (Salmen and Berrueta 2012). ROS such as H_2O_2 can enter into cells by crossing biological membrane through aquaporin channels (Bienert and Chaumont 2014). NOX 2 generally produces $O_2^{\cdot-}$, while cells expressing NOX 4 show detectable levels of H_2O_2 rather than $O_2^{\cdot-}$.

HIV proteins such as Vpr and Tat have been reported to perturb the miRNA expression in human microglial and neuronal cells (Mukerjee *et al.* 2011; Sun and Rossi 2011; Klase *et al.* 2012). In this study, we demonstrated the regulation of NOX2 and NOX4 through miR-17. The expression of miR-17 was attenuated by HIV-1 Tat C, which led to increased expression of NOX2, NOX4, and thereby ROS generation in human microglial cells.

Materials and methods

Cell culture

Human microglia clone 3 cell lines (HMC3) (Janabi *et al.* 1995) were obtained from Dr Karl-Heinz Krause, Department of Pathology and Immunology, Faculty of Medicine, University of Geneva, Switzerland as a kind gift. HMC3 cells were cultured in Dulbecco's modified Eagle's medium (DMEM, #12100-046; Invitrogen, Carlsbad, CA, USA) supplemented with 10% fetal bovine serum (#16000-044; Invitrogen), 100 U penicillin, and 100 μg/mL streptomycin (#10378016; Invitrogen). CEM-GFP cells (reporter T cell line) (NIH-AIDS Reagent Program, Germantown, MD, USA) were cultured in RPMI 1640 (23400-021; Gibco-BRL, Gaithersburg, MD, USA) with 10% fetal bovine serum, 100 U penicillin, and 100 μg/mL streptomycin. CEM-GFP cells were used for transactivation assay of HIV-1 Tat protein. HeLa cells were cultured in DMEM supplemented with 10% fetal bovine serum, 100 U penicillin, and 100 μg/mL streptomycin for Luciferase assay. HMC3 cells were cultured in white bottom 96-well plates (#3917; Corning Inc, New York, NY, USA) for ROS detection by fluorimetry. HMC3 cells were cultured in 12-well culture plates for ROS imaging experiments. All the cultures were incubated in humidified atmosphere (5% CO_2) at 37°C.

Expression and purification of HIV–1 Tat C protein

HIV-1 Tat C gene was amplified from HIV-1-infected cells and was cloned in pET-21b bacterial expression vector with His-tag attached to Tat at C-terminal. It was transformed in BL21 (DE3) cells, which were cultured in Luria Broth (LB) and induced by isopropyl-β-D-thio-galactosidase (IPTG) for 3 h for protein expression. Bacterial cells were pelleted and resuspended in 20 mL of lysis buffer (50 mM phosphate buffer pH 7.9, 0.4 mM EDTA pH 8, 300 mM KCl, 10 mM imidazole, 0.2 mM phenylmethanesulphonyl fluoride, 1 mM dithiothreitol, 0.1% tritonX-100). Cells were lysed by sonication and lysates were further used for purification. His-tagged recombinant HIV-1 Tat C protein was purified by affinity chromatography using nickel-nitrilotriacetic acid (Ni-NTA columns). Lysate was incubated with Ni-NTA column overnight at 4°C. Protein was eluted in elution buffer (Phosphate buffer pH 8, 300 mM imidazole) and was used for removal of imidazole in centrifugal concentrator (Amicon MWCO 3 kDa, UFC900396; Millipore Corporation, Bedford, MA, USA). Imidazole removal buffer (30 mM phosphate buffer, 70 mM KCl, 1 mM dithiothreitol) was used for concentrating the protein and aliquots were stored at −80°C for further experimental use. The expression and purification steps of this Tat$_{1-101}$ (11.51 kDa) were followed as per our standardized proto-

cols, protein was tested for its endotoxin levels, checked for its functional activity, and confirmed by western blotting as described in our previous reports (Mishra *et al.* 2012; Mishra and Singh 2013). Similarly, Tat protein of HIV clade B (Tat B) was cloned and purified.

MicroRNA target prediction

miR-17 was found to potentially target NOX2 and NOX4 3′UTR; as predicted by bioinformatic prediction tools: Pictar (MDC, Berlin, Germany), Target Scan 5.2 (Whitehead Institute of Biomedical Research, MIT, Boston, USA) and MicroRNA.org. 3′UTR binding sites of miR-17 in NOX2 and NOX4 were identified using TargetScan (version 5.2; http://www.targetscan.org).

HIV-1 Tat C treatment on HMC3 cells

HMC3 cells were grown till confluency and treated with HIV-1 Tat C protein at concentration of 1 μg/mL in serum-free DMEM media for various time points (0, 6, 12, and 24 h). Cells were harvested at time points as described above and used for RNA and protein extraction. HMC3 cells were treated with same doses of HIV-1 Tat C protein for similar time points for the ROS detection by fluorimetry. HMC3 cells were stained by 2′,7′ dichlorofluorescein diacetate (DCFDA) (#D6883 – 250 mg; Sigma-Aldrich, St Louis, MO, USA) and fluorescence was measured at 485/515 nm wavelength by EnSpire multimode plate reader. (PerkinElmer, Waltham, MA, USA). HMC3 cells were treated with same dose of HIV-1 Tat C protein for 24 h and stained by DCFDA for ROS imaging experiments.

RNA isolation and miRNA assay

RNA isolation was done with miRNeasy kit (#217004; Qiagen, Valencia, CA, USA) as per manufacturer's instruction. miRNA-specific primers and TaqMan reverse transcription kit (#4366596; Applied Biosystems, Warrington, UK) were used for cDNA synthesis. The conditions of PCR amplification were 16°C for 30 min, 42°C for 30 min, and 85°C for 5 min. miRNA assays were performed by quantitative PCR (qPCR) using miRNA-specific TaqMan probes (miR-17 Assay ID: 002308; miR-101 Assay ID: 002253; RNU24 Assay ID: 001001, #4427012, Applied Biosystems) and universal PCR master-mix (#4324018; Applied Biosystems). qPCR conditions for the amplification were 95°C for 10 min, 40 cycles of 95°C for 15 s, and 60°C for 60 s on ABI thermal cycler 7900 (Applied Biosystems, Foster City, CA, USA) and Roche LightCycler 480 II (Roche diagnostics, Switzerland).

Western blot analysis

Cell pellets were lysed with ristocetin-induced platelet agglutination buffer (150 mM NaCl, 50 mM Tris-HCl, pH 7.5, 1% NP-40, 0.5% sodium doxycholate, 0.1% sodium dodecyl sulfate, 1× protease inhibitor cocktail (GBiosciences, St Louis, MO, USA). Protein concentration was determined using Bradford assay (#500-0006; Bio-Rad Laboratories, Hercules, CA, USA). Equal amount of protein was run on 12% sodium dodecyl sulfate gel. Proteins were transferred onto polyvinylidene fluoride membrane (# IPVH00010; Millipore) at 100 V for 2 h. The blocking of membrane was done with 5% skimmed milk solution for 1 h followed by incubation in primary antibody for overnight. Membranes were washed with Tris-buffered Saline with Tween 20 buffer three times for 15 min each

and incubated with secondary antibody (1 : 50 000) for an hour. Membranes were given three washes again with Tris-buffered Saline with Tween 20 buffer and developed using Super Signal developing reagent (#34095; Pierce, Rockford, IL, USA). Antibodies against NADPH-oxidase 2 (gp91phox, #5653-1; Epitomics), NADPH-oxidase 4 (#3187-1; Epitomics-Abcam, Burlingame, CA, USA), and β tubulin (#ab6046; Abcam, Cambridge, MA, USA) have been used to study the expression levels of respective genes via western blotting.

MicroRNA over–expression

HMC3 cells were seeded and grown till 40–50% confluency. Transfection mixtures were prepared in low serum Opti-MEM media (#11058-021; Ambion, Foster City, CA, USA) and transfection was carried out using antibiotic-free media. Over-expression of miR-17 was done by transfecting 100pM miR-17 oligos (BioServe, Mallapur, Hyderabad, India) (sequence mentioned in Table 1) with Lipofectamine 2000 (#11668-019; Invitrogen). 100pM scramble miR-17 (sequence given in Table 1) was transfected in HMC3 cells as negative control. Over-expression of miR-101 was performed by transfecting 100pM of miR-101 oligos (sequence mentioned in Table 1) as non-target control. After 48 h, the over-expression of miRNAs was confirmed by qPCR using respective TaqMan probes. The expression levels of NOX2 and NOX4 were checked by western blot analysis.

MicroRNA inhibition

Cellular miR-17 was inhibited by transfecting HMC3 cells with 100pM of anti-miR-17 (MH12412; Ambion) and Cy3-labeled negative control (anti-miR) with Lipofectamine 2000 for 48 h. Transfection efficiency was determined by visualizing Cy3-labeled anti-miR fluorescence in transfected control HMC3 cells. The levels of expressions of NOX2 and NOX4 protein expressions were analyzed by western blot analysis in anti-miR-17-transfected cells.

Site-directed mutagenesis

As per the bioinformatic analysis, three sites (7-mer, 6-mer, and 5-mer) of miR-17 binding in 3′UTR of NOX2 and three sites (all 7-mer) in NOX4 3′UTR were predicted. Complementary binding sequences GCACTTT were deleted from sites 195–201 (MUT1), GCACT from sites 1803–1808 (MUT2), and GCACTT from sites 2316–2322 (MUT3) in NOX2 3′UTR. However, the complementary binding sequences GCACTTT were deleted from sites 988–994 (MUT1), 1191–1197 (MUT2), and 1369–1375 (MUT3) in NOX4 3′UTR, The mutants were created by site-directed mutagenesis using primers listed in Table 2. PCR was carried out using 50 ng plasmid template, 0.3 μM primers in Phusion High-Fidelity master mix buffer (#M0531; New England Biolabs, Ipswich, MA, USA) at

Table 1 RNA oligo sequences

Name	Sequence 5′-3′
miR-17 oligos	CAAAGUGCUUACAGUGCAGGUAG
miR-101 oligos	UACAGUACUGUGAUAACUGAA
miR-17 scramble	GGGGUCUCCAUCCUCACUCUCAG

Table 2 List of primers

Gene name	Direction	Primer sequence (5′-3′)
WT NOX2 3′UTR	Forward	ATACTCGAGCTTGTCTCTTCCATGAGGAAATAAATG
	Reverse	ATTAATTAGCGGCCGCGAAAGCTCATTCATTTTAATAG
MUT 1 NOX2 3′UTR	Forward	GGTTTTGAGATACAA ACATTATTTC
	Reverse	GAAATAATGTTTGTATCTCAAAACC
MUT2 NOX2 3′UTR	Forward	ATCCTCAGGGAGGGTAGGTC
	Reverse	GACCTACCCTCCCTGAGGAT
MUT3 NOX3 3′UTR	Forward	TTTTTTTTTTAAGTATTTAGCATTT
	Reverse	AAATGCTAAATACTTAAAAAAAAAA
WT NOX4 3′UTR	Forward	GAATTCAAACTTTTGCCATGAAGC
	Reverse	CTCGAGCAATTTTAACATTTATTGCT
MUT 1 NOX4 3′UTR	Forward	ATAGTTAGTTAATTTGAGACCAAAGGACAT
	Reverse	ATGTCCTTTGGTCTCAAATTAACTAACTAT
MUT2 NOX4 3′UTR	Forward	ATATTACTGTCTTGGTATCCTG
	Reverse	CAGGATACCAAGACAGTAATAT
MUT3 NOX4 3′UTR	Forward	AATCCCGGGGAGGCCAAGGCA
	Reverse	TGCCTTGGCCTCCCCGGGATT
GAPDH	Forward	ATGGGGAAGGTGAAGGTCG
	Reverse	GGGGTCATTGATGGCAACAATA
TNF-α	Forward	CCTCTCTCTAATCAGCCCTCTG
	Reverse	GAGGACCTGGGAGTAGATGAG
IL-1β	Forward	AGCTACGAATCTCCGACCAC
	Reverse	CGTTATCCCATGTGTCGAAGAA
IL-6	Forward	ACTCACCTCTTCAGAACGAATTG
	Reverse	CCATCTTTGGAAGGTTCAGGTTG

98°C for 2 min, 40 cycles at 98°C for 30 s, 47°C for 30 s, 72°C for 2 min 30 s, and final extension at 72°C for 10 min. Mutant 3′UTR was constructed using these mutated fragments (MUT1, MUT2, and MUT3) through recombination PCR, was further cloned in psiCHECK-2 vector. These mutants were then used as set of negative controls for Luciferase assay.

Luciferase reporter assay

Luciferase reporter clones of intact sequences WT NOX2 3′UTR (cloned in psiCHECK-2 Vector, #C8021; Promega, Madison, WI, USA), WT NOX4 3′UTR (#HmiT054569-MT01; GeneCopeia), mutant-NOX2 3′UTR clone, and mutant-NOX4 3′UTR clones were cotransfected individually with miR-17 oligos in HeLa cells. Luciferase assay was performed after 24 h of transfection using luciferase assay kit (#E4030; Promega). β-galactosidase assay has been performed (#E2000; Promega) for normalization, according to the manufacturer's protocol. Samples were read using multimode plate reader (EnSpire, PerkinElmer).

Intracellular ROS detection

HMC3 cells were seeded in 96-well bottom plates and were allowed to adhere overnight. Cells were treated with 1 µg/mL concentration of HIV-1 Tat C protein upon confluency, for different time points. Cells were washed and stained with 5 µM DCFDA (#D6883-250 mg; Sigma-Aldrich) for 15 min at 37°C. Cells fluorescence was measured at 480 nm/535 nm on multimode plate reader (EnSpire, PerkinElmer) at each time point. Cells were stained and incubated with same concentration of DCFDA, washed with phosphate-buffered saline, and images were captured by Zeiss Axiocam MRC

fluorescent microscope (Carl Zeiss, Gottingen, Germany) for imaging experiment of intracellularly generated ROS. ROS measurement was done in cells after over-expressing miR-17 and inhibiting miR-17. Cells were seeded in 96-well plates and ROS levels were checked after 12 h of transfections. In the experiments of over-expression followed by HIV-1 Tat C treatment and HIV-1 Tat C treatment alone, cells were treated with HIV-1 Tat C protein after 6 h of seeding of cells in 96-well plates. The HMC3 cells exposed to HIV-1 Tat C protein for 24 h were used for DCFDA staining and fluorescence measurement.

Expression of cytokines and evaluation of miR–17 expression levels in HMC3 cells exposed to different stimuli

Cytokine levels in cells over-expressing miR-17 and cells in which miR-17 was inhibited were determined through quantitative PCR. RNA was isolated (as mentioned above) from cells transfected with scramble miR-17, miR-17 oligos, Cy3, and anti-miR-17. Two micrograms of RNA was converted into cDNA using Superscript II reverse transcriptase system (#11904-018; Invitrogen) according to the manufacturer's protocol. Two hundred nanograms of cDNA was then used to perform quantitative/RT-PCR using SYBR Green Supermix (#4367659; Applied Biosystems). Expression levels of TNF-α, IL-1β, and IL-6 were determined using cytokine-specific primers (Table 2) and Glyceraldehyde 3 phosphate dehydrogenase (GAPDH) was used as internal control. To demonstrate the specificity of miR-17 expression in response to HIV-1 Tat C protein, we exposed HMC3 cells with different cell stimulants such as HIV-1 Tat B (recombinant Tat B protein), lipopolysaccharide (LPS, Sigma-Aldrich), and bovine serum albumin (BSA, #NEB

B9001) each with 1 μg/mL concentration for 24 h. RNA was isolated from the harvested cells to determine the expression pattern of miR-17 using miR-17-specific TaqMan primers and probes.

Statistical analysis

All the data are plotted as mean ± SE. Student's *t*-test was used for two-group comparison, multiple group comparisons were performed by one-way ANOVA, where *p*-values were determined by the Turkey–Kramer multiple comparison *post hoc* test. miRNA expression level changes have been shown as fold changes compared to control/untreated cells.

Results

HIV-1 Tat C treatment decreases the expression level of miR-17 in HMC3 cells

We studied the changes in expression level of miR-17 in HMC3 cells exposed to HIV-1 Tat C protein at various time points. Real-time quantitative (qPCR) analysis with TaqMan microRNA assay specific to miR-17 showed that mature miR-17 levels significantly decreased upon HIV-1 Tat C exposure at 6, 12, and 24 h (Fig. 1b) compared to 0-h control. The miR-17 levels were significantly decreased at 6 h (34% decrease), 12 h (24% decrease), and at 24 h (54% decrease) ($p \leq 0.05$), compared to untreated control cells.

HIV-1 Tat C treatment induces expression level of NOX2 and NOX4 in HMC3 cells

To study the effect of HIV-1 Tat C on NOX2 and NOX4 expression in HMC3 cells, we determined the levels of their expressions at 0, 6, 12, and 24 h after HIV-1 Tat C treatment (Fig. 1a). HIV-1 Tat C exposure for the above-mentioned time points resulted into increased expression of NOX2 and NOX4. A significant increase in NOX2 expression level was observed within each time-point interval, compared to controls, (Fig. 1c). NOX2 expression was increased by twofolds at 6 h (**$p \leq 0.01$), 3.2 folds at 12 h (***$p \leq 0.001$), and maximum of fivefolds at 24 h (***$p \leq 0.001$), as compared to controls. Steady increase in NOX4 expression was noted with 1.5 folds higher at 6 h, 1.75 folds at 12 h (*$p \leq 0.05$), and highest of 2.6 folds at 24 h (*$p \leq 0.05$), as compared to controls. Significant changes between the time intervals of 6–24 h (##$p \leq 0.01$) were also observed (Fig. 1d).

miR-17 directly binds to 3′UTRs of NOX2 and NOX4

miRNAs contain 2–8 nt seed region, having complementarity with their 3′UTR of target mRNAs. MicroRNAs regulate the expression levels of target genes post-transcriptionally, either by repression of translation or by degrading target mRNA. We detected reduced levels of miR-17 on HIV-1 Tat C
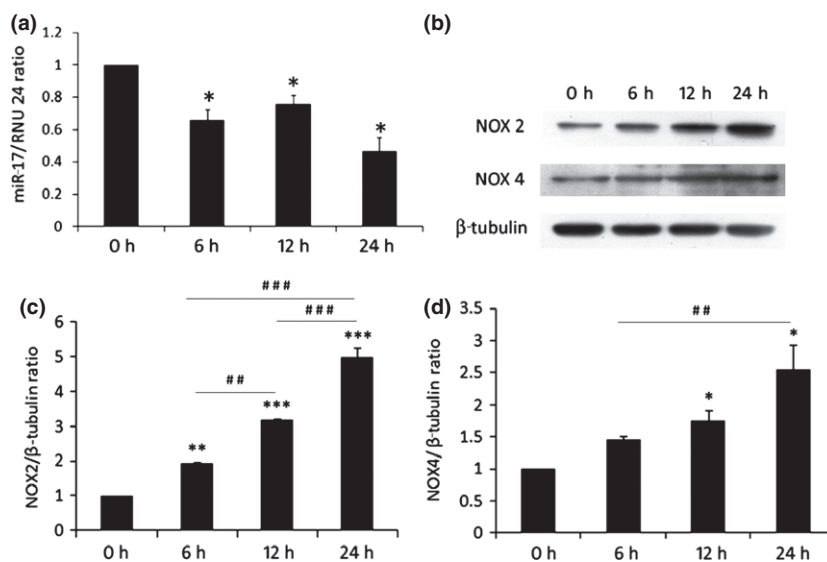

Fig. 1 HIV-1 Tat C decreases miR-17 expression and increases NOX2 and NOX4 expression in HMC3 cells. (a) Fold change in miR-17 levels in HMC3 cells after Tat C treatment at 0, 6, 12, and 24 h time points. miR-17 levels were detected by qPCR with TaqMan hsa-miR-17 assay. Expression levels were normalized by small RNA, RNU24 and were found to be statistically significant (*$p \leq 0.05$). (b) Western blots images showing NOX2 and NOX4 expression levels at 0, 6, 12, and 24 h after Tat C treatment. (c) The graph bars are showing densitometry analysis of NOX2 western blots normalized by β-tubulin using ImageJ software. Statistical significance indicated by, **$p \leq 0.01$, ***$p \leq 0.001$, respectively as compared to 0h control. Changes in expressions at 12 and 24 h were statistically significant with 6 h, shown as ##$p \leq 0.01$, ###$p \leq 0.001$, respectively, and 12 h with 24 h ###$p \leq 0.001$. (d) The graph is showing densitometry of NOX4 normalized by β-tubulin and statistical significance shown as ##$p \leq 0.01$. All the experiments are repeated three times and are represented as mean ± SE.
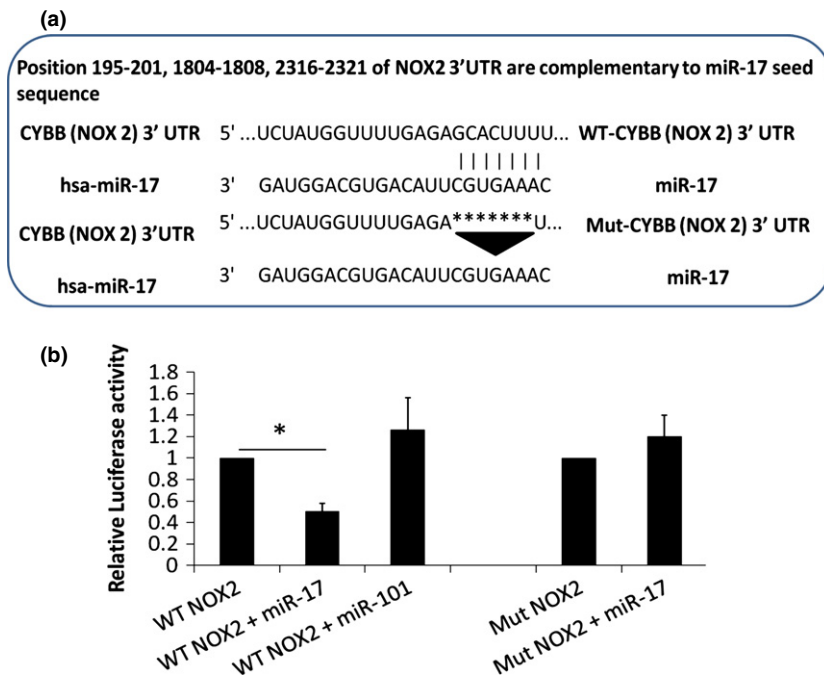
(a)

(b)

Fig. 2 miR-17 directly targets NOX2 3′UTR (untranslated regions). (a) Schematic showing 7-mer complementary binding of miR-17 at site 195–201 to NOX2 3′UTR and 4-mer and 5-mer binding at 1804–1808 and 2316–2321, respectively. Hela cells were cotransfected with WT-NOX2 3′UTR reporter constructs, Mut-NOX2 reporter clone, and miR-17 oligos and miR-101 as non-specific miRNA control for luciferase assay. (b) The graph is showing 50% decrease (*$p \leq 0.05$) in luciferase activity in WT-NOX2 and miR-17-transfected cells and no significant change in luciferase activity in Mut-NOX2 reporter construct and miR-17 transfected cells. All experiments are repeated three times and are represented as mean ± SE.

treatment at 6, 12, and 24 h time points (Fig. 1a). Bioinformatics tools were used to analyze the binding of miR-17 with NOX2 and NOX4. 3′UTR of NOX2 and NOX4 showed strong and multiple binding sites for miR-17. To confirm the miRNA binding, we performed luciferase assay, where HeLa cells were transfected with reporter construct of WT NOX2, NOX4 and mutant NOX2, NOX4 3′UTR. Only the WT 3′UTR constructs and miR-17 oligos cotransfected cells showed reduced luciferase activity by 50% ($p < 0.05$) for NOX2 (Fig. 2) and by 38% ($p < 0.005$) for NOX4 (Fig. 3). To further confirm, the mutants of NOX2 and NOX4 were cotransfected with miR-17 oligos, which did not result into significant decrease in luciferase activity. miR-101 was also cotransfected with 3′UTR reporter constructs of NOX2 and NOX4 and no change was observed in luciferase activity, which indicated the specificity of binding of miR-17 with the 3′UTRs of their target genes NOX2 and NOX4 (Figs 2 and 3).

Over-expression of miR-17 suppresses the expression of NOX2 and NOX4

We confirmed that NOX2 and NOX4 had strong binding sites for miR-17 by luciferase reporter assay. The expression levels of NOX2 and NOX4 were analyzed in miR-17 over-expressed HMC3 cells and by western blotting analysis (Fig. 4b). Over-expression was confirmed by real-time PCR for miR-17-specific Taqman primer as probe (Fig. 4a). miR-17 was found to be over-expressed by 526.6 folds, compared to untransfected control (*$p \leq 0.05$) and scramble miR-17-transfected cells (#$p \leq 0.05$). miR-101 was also over-expressed as 21.6 folds compared to control (**$p \leq 0.01$),

to study the effect of non-specific miRNA (Fig. 4a). Increased levels of miR-17 in cells significantly down-regulated the expression of NOX2 by 65% as compared to control ($p \leq 0.005$) (Fig. 4c). NOX2 was significantly down-regulated in miR-17 over-expressing cells, compared to scramble miR-17 and non-specific miR-101 controls ($p \leq 0.01$, $p \leq 0.01$, respectively). The over-expression of miR-17 resulted into the significant decrease (~ 70%) in NOX4 expression, compared to control ($p \leq 0.005$) (Fig. 4d). NOX-4 was also significantly down-regulated compared to scramble miR-17 ($p \leq 0.005$) and non-specific miR-101 ($p \leq 0.05$).

Inhibition of miR-17 enhances the expression of NOX2 and NOX4

The HMC3 cells were transfected with anti-miR-17 to inhibit the cellular mature miR-17 and to study the knockdown effect of miR-17 on the expression levels of NOX2 and NOX4. Inhibition of miR-17 was confirmed by qPCR using miR-17 specific TaqMan probes (Fig. 5a). Anti-miR-17-transfected HMC3 cells showed the significant inhibition of mature miR-17 by 87% as compared to control (**$p \leq 0.01$) and Cy3 control (#$p \leq 0.05$). Expression levels of NOX2 and NOX4 were checked by western blotting (Fig. 5b). Increase in NOX2 expression [2.9 folds (*$p \leq 0.05$)] (Fig. 5c) and NOX4 [2.5 folds (**$p \leq 0.01$)] was observed in anti-miR-17-transfected HMC3 cells, as compared to controls (Fig. 5d). These changes were statistically significant compared to Cy3 controls (#$p \leq 0.05$, #$p \leq 0.05$, respectively). HIV-1 Tat C exposure showed similar reduction in miR-17 levels and reflected similar trends in the expression levels of

(a)

Positions 988-994, 1191-1197, 1369-1375 of NOX4 3'UTR are complementary to miR-17 seed sequence.

| NOX 4 3'UTR | 5' | ...ACGCCUGUAAUCCCGGCACUUUG... | WT-NOX 4 3'UTR |
| hsa-miR-17 | 3' | GAUGGACGUGACAUUCGUGAAAC | miR-17 |

| NOX 4 3'UTR | 5' | ...ACGCCUGUAAUCCC ******* G... | MUT-NOX 4 3'UTR |
| hsa-miR-17 | 3' | GAUGGACGUGACAUUCGUGAAA C | miR-17 |

Fig. 3 miR-17 directly targets NOX4 3'UTR (untranslated regions). (a) Schematic showing three perfect complementary binding sites 988–994, 1191–1197, and 1369–1375 of NOX4 3'UTR with miR-17. WT-NOX4 3'UTR reporter constructs and Mut-NOX4 reporter constructs were cotransfected with miR-17 oligos in Hela cells and miR-101 was used as non-specific microRNA control. (b) The graph is showing 62% decrease (**$p \leq 0.01$) in luciferase activity, in WT-NOX4 and miR-17 transfected cells while no significant change was seen in Mut-NOX4 reporter construct and miR-17-transfected cells and with non-specific miR-101 transfection. All experiments are repeated three times, represented as mean ± SE.
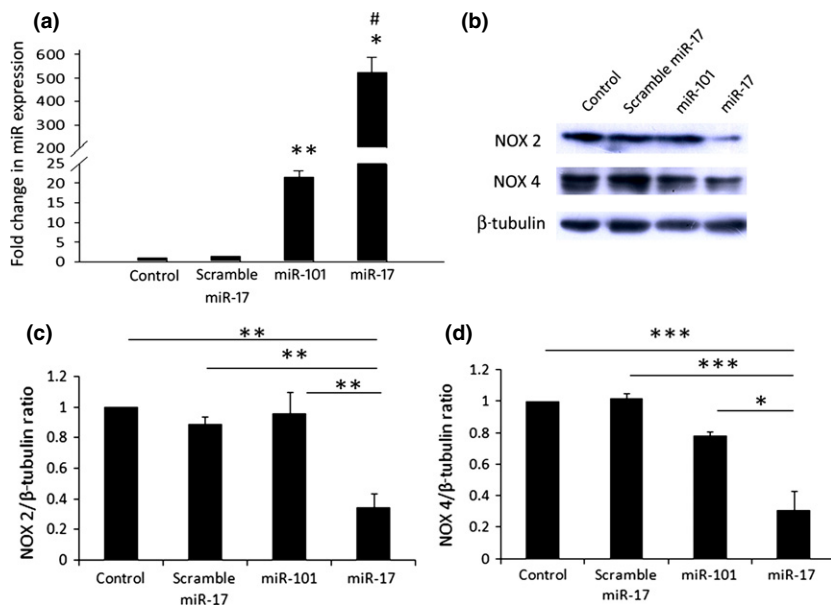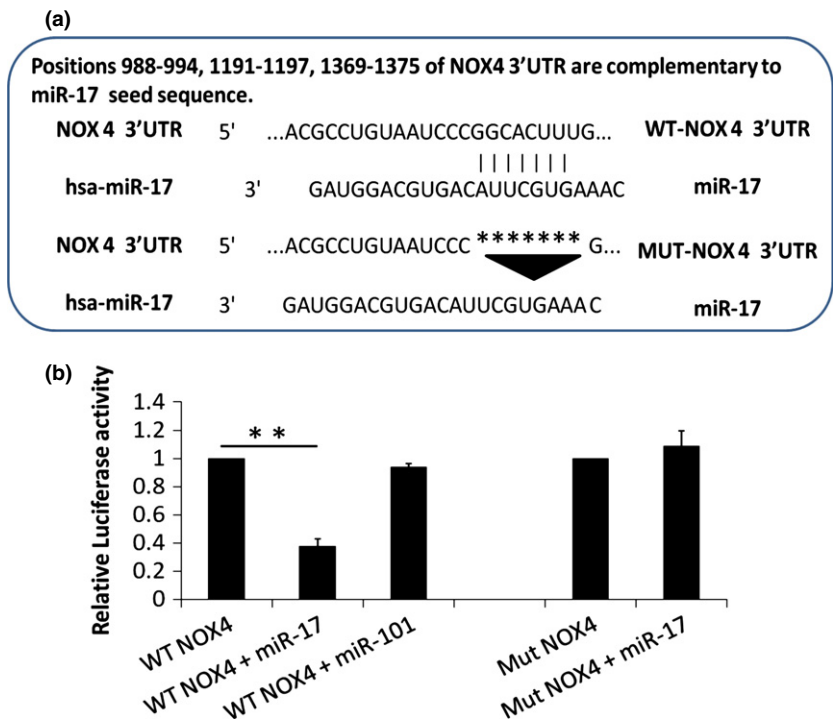
(b)

Fig. 4 Over-expression of miR-17 suppresses NOX2 and NOX4 expression in HMC3 cells. HMC3 cells were transfected with 100pM miR-17 oligos and as a control non-specific miR-101 and scramble-miR-17 were transfected. (a) Over-expression was confirmed with qPCR with TaqMan probes specific to miR-17 and miR-101. miR-17 was over-expressed by 526.6 folds as compared to control (*$p \leq 0.05$) and was also significant as compared to scramble miR-17 (#$p \leq 0.05$). miR-101 is also over-expressed by 21.6 folds as compared to control (**$p \leq 0.01$). (b) Western blots images showing NOX2 and NOX4 levels upon transfection of scramble miR-17, over-expression of miR-101 and miR-17 (c and d). Densitometry analysis of western blots for NOX2 and NOX4 expression. Significant decrease in NOX2 and NOX4 levels was found in comparison to all controls, untransfected, scramble-miR-17 and non-specific miR-101 (*$p \leq 0.05$, **$p \leq 0.01$,***$p \leq 0.001$) and no change was observed when scramble miR-17 and non-specific miR-101 were transfected. All experiments were performed in sets of three and data are presented as mean ± SE of three independent experiments.
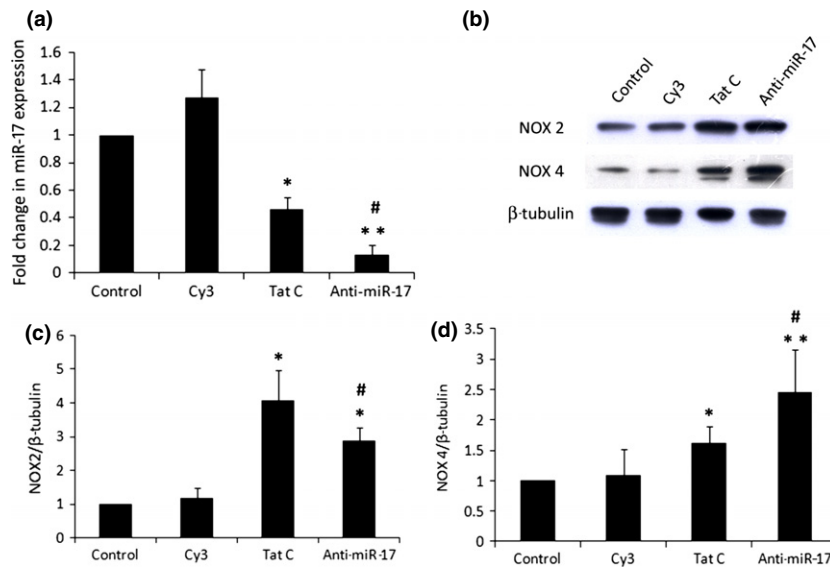
Fig. 5 Knockdown of miR-17 rescues NOX2 and NOX4 expression in HMC3 cells. HMC3 cells were transfected with anti-miR-17 inhibitor to knock down miR-17 in cells and its effect on expression level of NOX2 and NOX4 was observed. Decline in levels of cellular miR-17 was confirmed by qPCR using miR-17-specific TaqMan probes. Cy3 was used as negative control. (a) Graphical representation of mature miR-17 levels quantified by qPCR, upon Tat C treatment and knocking down of miR-17. A significant decrease (54%) in miR-17 levels was observed upon Tat C treatment as compared to untransfected control (*$p \leq 0.05$) and Cy3-negative control ($^{\#}p \leq 0.05$). Knockdown of miR-17 is showing almost 87% decrease, significant as compared to control (**$p \leq 0.01$) and Cy3-transfected-negative control ($^{\#}p \leq 0.05$). (b) Western blots images showing NOX2 and NOX4 expression levels in Tat C-treated and miR-17 knocked down samples as compared to control and Cy3-negative control. (c and d) Graphical representation of NOX2 and NOX4 expression level after densitometry analysis showing significant increase by fourfolds in Tat C treatment as compared to control (*$p \leq 0.05$) and as compared to Cy3 ($^{\#}p \leq 0.05$) and by 2.9 folds in anti-miR-17-transfected samples. All the experiments are repeated three times and are represented as mean ± SE and statistical significance shown as $^{\#}p \leq 0.05$.

NOX2 and NOX4. NOX2 expression increased by fourfolds, whereas NOX4 expression was increased by 1.7 folds (*$p \leq 0.05$, *$p \leq 0.05$, respectively).

Over-expression of miR-17 decreases intracellular ROS production in HMC3 cells

Whether miR-17 directly has any effect on intracellular ROS production; ROS levels were studied by over-expressing miR-17 in HMC3 cells. The abundance of miR-17 in HMC3 cells could reduce ROS levels close to normal. Scramble miR-17 and non-specific miR-101 were used as controls and did not show any significant change in ROS levels (Fig. 6c). Any significant increase was not observed in the levels of ROS in miR-17 over-expressing HMC3 cells exposed to HIV-1 Tat C, as observed in HMC3 cells exposed to HIV-1 Tat C protein alone (fold change 1.22 folds, $p \leq 0.01$) (Fig. 6c). This demonstrated that miR-17 regulates the intracellular ROS levels through direct targeting of NOX2 and NOX4.

HIV-1 Tat C induces intracellular ROS level

NADPH oxidases are the major sources of ROS, generation especially in glial cells. As miR-17 was down-regulated upon HIV-1 Tat C treatment and NOX2 and NOX4 were elevated, we checked intracellular ROS production at 0, 6, 12, and 24 h. ROS levels were checked by fluorimetry in DCFDA-stained HMC3 cells. Significant increase in ROS generation was observed at each time point with highest of 1.16 folds at 24 h ($p \leq 0.01$) (Fig. 6a). This was also confirmed by imaging analysis of HIV-1 Tat C exposed HMC3 cells at 24 h. Image analysis showed the increased intensity of DCFDA-stained cells and enhanced production of ROS as compared to controls (Fig. 6b). Zero-hour control showed no ROS production (Fig. 6bi). Control cells were kept in incomplete DMEM for 24 h and stained by DCFDA. There was no significant ROS production in control cells (Fig. 6bii); however, the HMC3 cells exposed to HIV-1 Tat C protein for 24 h have shown significant ROS production (Fig. 6biii).

Anti-miR-17 elevates intracellular ROS levels

miR-17 regulates the expression of NOX2 and NOX4 by binding to their 3′UTRs. Inhibition of miR-17 resulted in enhanced expression of NOX2 and NOX4. To study if reduction in miR-17 levels affects intracellular ROS production, the ROS levels were measured in cells transfected with
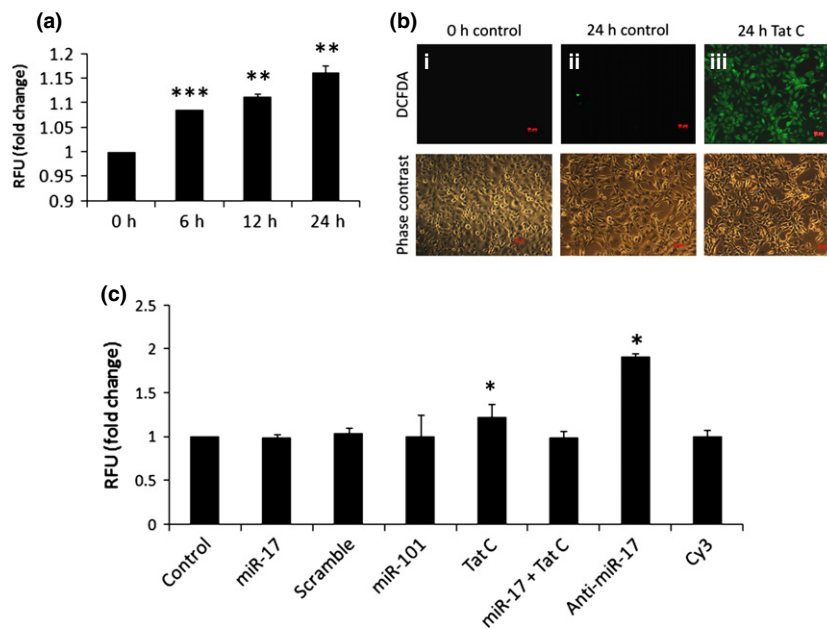
Fig. 6 HIV-1 Tat C induced increase in intracellular ROS levels mediated by miR-17. (a) HMC3 cells were treated by Tat C for 6, 12, and 24 h and 0 h was control and cells were stained by 2′,7′ dichlorofluorescein diacetate (DCFDA) followed by fluorimetry analysis by excitation at 480 nm and emission at 535 nm. Graphical presentations depicting fold change in ROS levels, indicating a gradual increase in ROS at 6 h (***$p \leq 0.005$), 12 h (**$p \leq 0.01$), and maximum of 1.16 folds at 24 h (**$p \leq 0.01$) as compared to 0-h control. (b) Microscopic image showing an increase in fluorescence because of ROS at 24 h (iii) as compared to 0-h control (i) and 24-h control [cells in incomplete Dulbecco's modified Eagle's medium (DMEM)] (ii). Lower panel shows respective phase contrast images of above panel. (c) The graph bars are showing the change in ROS levels, as compared to untransfected/untreated control (*$p \leq 0.05$). No changes in ROS were observed after transfecting scramble miR-17, non-specific miR-101, and Cy3-negative control. All the experiments were repeated independently three times, each set in quad-replicates. Data are represented as mean ± SE.

anti-miR-17 (miR-17 inhibitor). ROS production was increased by 1.9 folds ($p \leq 0.01$) in HMC3 cells as compared to controls upon inhibiting miR-17. Cy3 was used as negative control and showed no change in ROS levels (Fig. 6c). This trend corroborated with increase of ROS found in HIV-1 Tat C-treated cells. We demonstrated that miR-17 directly regulates the expression of NOX2 and NOX4 and thus its downstream function in terms of intracellular ROS production.

Increased ROS leads to microglial activation and HIV–1 Tat C specifically modulates miR–17 levels in HMC3 cells

Reduced levels of miR-17 resulted in increased expression of NOX2 and NOX4 as a result of elevated levels of intracellular ROS levels. To study the effect of ROS on the expression of cytokines, the expression levels of cytokines were estimated by real-time PCR. TNF-α (Fig. 7a) was increased by 5.6 folds, IL-1β (Fig. 7b) increased by 1.8 folds ($p \leq 0.05$), and IL-6 (Fig. 7c) approximately 22 folds ($p \leq 0.01$) in miR-17-inhibited cells as compared to Cy3 control. All three cytokines were found to be suppressed in the cells over-expressing miR-17, compared to controls (transfection control scramble miR-17). This indicated that elevated ROS levels led to increased cytokine expression through activated microglial cells. To check the effect of

different stimuli on miR-17 levels, we treated HMC3 cells with BSA, HIV-1 Tat B and LPS. RT-PCR revealed no significant change in miR-17 levels (Fig. 7d). This observation suggested that decreased expression of miR-17 affected downstream NOX2, NOX4, and ROS specifically in response to HIV-1 Tat C.

Discussion

HIV-1 infection extends into cognitive and motor dysfunctions collectively termed as HIV-associated neurological disorders. Neuroinflammation is either caused by direct infection of virus to the permissive neuronal cells (astrocytes or microglia) or by exposure of the cells to extracellularly secreted viral proteins like Tat, Vpr, Nef etc.

ROS generated by phagocytic cells have primary function of destroying microbes. However, it has secondary role in modulating redox signaling pathways (Thannickal and Fanburg 2000). ROS can lead to reversible chemical modifications in various transcription factors [NF-κB (nuclear factor kappa-light-chain-enhancer of activated B cells), redox-sensitive transcription family] affecting their functions and thus influencing the inflammatory responses of human microglial cells (Forman and Torres 2001). ROS,
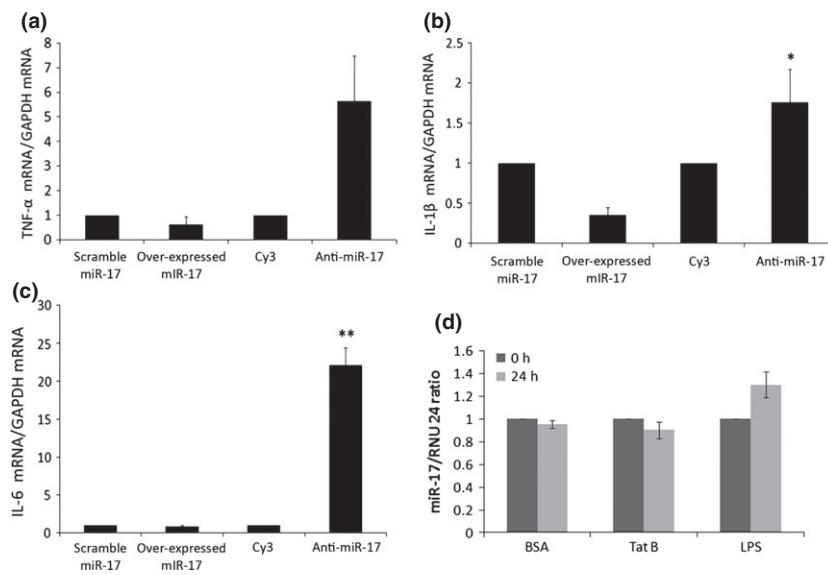
Fig. 7 HMC3 cells activation through ROS and specificity of miR-17 expression to HIV-1 Tat C treatment. HIV-1 Tat C suppresses miR-17 levels in HMC3 cells resulting in induction of NOX2 and NOX4 expression and thus ROS levels. To study whether increased intracellular ROS resulted into increased expression of cytokines, the levels of proinflammatory cytokines were determined in cells over-expressing miR-17 and in cells with miR-17 inhibition, by RT-PCR. (a) Levels of TNF-α were found to be less than control (scramble miR-17) in cells over-expressing miR-17. In cells transfected with Anti-miR-17, TNF-α levels increased by 5.6 folds as compared to Cy3 control. (b) IL-

1β levels reduced in cells over-expressing miR-17 and were induced by approximately 1.8 folds in miR-17-inhibited cells (*$p \leq 0.05$). (c) IL-6 levels increased by approximately 22 folds (**$p \leq 0.01$) as compared to Cy3 control in anti-miR-17-transfected cells and suppressed in cells over-expressing miR-17, compared to scramble miR-17-transfected cells. To study the specificity of miR-17 expression to HIV-1 Tat C treatment, HMC3 cells were exposed to bovine serum albumin (BSA), HIV-1 Tat B and lipopolysaccharide (LPS) and miR-17 levels were determined after 24 h of treatment. (d) None of the treatments showed any significant change in miR-17 levels at 24 h.

produced during oxidative stress by activated microglial cells, may result in neuronal damage (Ghosh *et al.* 2014; Xing *et al.* 2014).

HIV infection modulates the miRNA expression pattern of the infected cells (Yeung *et al.* 2005). miR-17 has been reported to target P300/CBP-associated factor, a Tat transcriptional cofactor required for HIV replication and establishing HIV latency (Triboulet *et al.* 2007). miR-17 has been reported to be down-regulated by twofolds in HIV-infected CEMx174 cells (Hayes *et al.* 2011).

Therefore, the levels of miR-17 were checked in HMC3 cells in response to HIV-1 Tat C protein. miR-17 was found to be down-regulated at early time points of HIV-1 Tat C protein exposure. Chronically activated microglial cells have been reported to secrete out neurotoxic factors, which could result in neuronal damage (Chao *et al.* 1992; Frank-Cannon *et al.* 2009). HIV Tat is known to activate microglial cells, leading to free radical stress (Turchan-Cholewo *et al.* 2009a). Microglial cells express NOXs, which play a major role in ROS production pathway. miR-17 has one strong binding site in 3′UTR of NOX2 and three binding sites in 3′UTR of NOX4. The down-regulation of miR-17 has been reported in kidneys of diabetic nephropathy (DN) patients with increased NOX4 levels (Fu *et al.* 2010).

HIV-1 Tat B exposed SH-SY5Y (neuronal cell line) and HN (primary human neurons) cells have shown the differential expression pattern of microRNAs. Tat B has been reported to induce miR-34a in SH-SY5Y cells, which targeted cAMP-response element binding protein, a neuroprotective protein (Chang *et al.* 2011). The increased expression of miR-1 has been reported in neurons exposed to HIV Tat protein. The miR-1 regulates Mef2A, further regulating the miR (379–410) cluster responsible for dendritogenesis (Fiore *et al.* 2009). HIV Tat exposure to neuronal cells results in the inhibition of miR-128a, which regulates the expression of pre-synaptic protein SNAP25 (Eletto *et al.* 2008). We previously reported perturbation in microRNAs in brain microvascular endothelial cells and microglial cells upon Tat C exposure. miR-32 affected expression of inflammatory genes by targeting TRAF3 in microglial cells upon Tat C exposure (Mishra *et al.* 2012). HIV-1 Tat C also induces miR-101 expression in brain microvascular endothelial cells, which targets VE-Cadherin and compromises blood–brain barrier integrity and permeability (Mishra and Singh 2013). We observed down-regulation in miR-17 levels and consequent increase in expressions of NOX2, NOX4 in HMC3 cells exposed to HIV-1 Tat C. In addition, we studied the effect of increased

NOX expression on ROS production. The ROS increased gradually within 24 h of HIV-1 Tat C exposure in HMC3 cells. The fluorimetry data and image analysis showed the maximum levels of ROS production at 24 h.

The luciferase assay demonstrated the direct binding of miR-17 to the 3′UTR of NOX2 and NOX4 genes. The luciferase reporter assay performed in cotransfection experiments with miR-17 demonstrated the direct binding of miR-17 to 3′UTR of NOX2 and NOX4. The deletion mutant 3′UTR of NOX2 and NOX4 devoid of complementary binding sites for seed region of miR-17 could not show any reduction in luciferase activity. Reduction in luciferase activity was more in NOX4 than NOX2, which could be due to three perfect 7-mer binding sites of miR-17 in 3′UTR of NOX4 and presence of only one perfect 7-mer binding site in 3′UTR of NOX2.

The ROS generation has been reported during various viral infections. HCV increases ROS production by inducing NOX4; which results in oxidative stress (Boudreau *et al.* 2009). HSV has been reported to produce ROS through NOX, which induces cytokine expression in microglial cells, resulting in neuronal damage (Hu *et al.* 2011). To determine the specificity of post-transcriptional regulation of NOX2/ NOX4 genes by miR-17, we inhibited cellular miR-17 in HMC3 cells and observed the expression patterns of NOX2, NOX4 along with intracellular ROS production. Both the miR-17 inhibition and HIV-1 Tat C exposure resulted in increased expression of NOX2/NOX4 and elevated intracellular ROS generation. These findings have established that HIV-1 Tat C induces the intracellular ROS generation via down-regulation of miR-17 in microglial cells.

The miR-17 was over-expressed in HMC3 cells to further validate the specificity of miR-17-mediated regulation of NOX2 and NOX4. The over-expression of miR-17 resulted in significant reduction in expression of NOX2 and NOX4. Over-expression of scrambled miR-17 and non-specific miR-101 showed no significant changes in NOX2 and NOX4 levels, thus confirming the specificity of miR-17-mediated regulation of the NOX2 and NOX4. The over-expression of miR-17 in HMC3 cells did not result in the reduction in ROS production, compared to controls. This indicated the redundancy in ROS generation pathway. In addition to miR-17, other pathways may also contribute to ROS production. Therefore, miR-17 over-expression did not result in the reduction of ROS production above the controls. HIV-1 Tat C exposure induced the levels of ROS production in HMC3 cells but cells over-expressing miR-17 followed by HIV-1 Tat C exposure did not show any significant increase in ROS production. This may be due to the higher levels of miR-17 in HMC3 cells (exogenous over-expression), which may nullify the effect of HIV-1 Tat C protein.

Increased NOX expression induces ROS, and that results in the microglial activation by secretion of pro-inflammatory cytokines and chemokines (Li *et al.* 2009a; Qin *et al.* 2013; Chantong *et al.* 2014). The elevated levels of NOX2 and

NOX4 were due to reduced expression of miR-17, which resulted in increased ROS production. ROS activates microglial cells, which leads to the expression of various proinflammatory cytokines. TNF-α, IL-1β, and IL-6 were found to be raised by several folds in HMC3 cells transfected with miR-17 inhibitor. Reduced levels of miR-17 resulted in increase in ROS, which in turn activated microglia and led to increased expression of cytokines. These cytokines were found to be suppressed in cells over-expressing miR-17, which demonstrated the miR-17-mediated regulation of ROS production and other downstream molecules by targeting NOX2 and NOX4. HIV Tat protein has been reported to induce the expression of cytokines and chemokines (Chen *et al.* 1997; Sheng *et al.* 2000; Williams *et al.* 2010; Jin *et al.* 2012) through NOX (Turchan-Cholewo *et al.* 2009b). The roles of cellular microRNAs have been reported in different disease models. miR-9 has been reported to target monocyte chemotactic protein-induced protein 1 during microglial activation in neurodegenerative diseases (Yao *et al.* 2014). miR-124 has been reported to target C/EBPα (CCAAT/enhancer-binding protein-α) in monocyte-lineage cells, deactivating macrophages by polarizing them from M1 to M2 and promoting microglial differentiation (Ponomarev *et al.* 2011). The role of miR-200b in microglial cells has been reported in neuroinflammation by modulating JNK (cJun N-terminal Kinase) and mitogen-activated kinases (Jadhav *et al.* 2014). miR-21 has been reported to regulate Fas ligand in hypoxia-mediated microglial activation, which leads to microglia-mediated neuronal apoptosis (Zhang *et al.* 2012). We have demonstrated that the modulation of miR-17 by HIV-1 Tat C in microglial cells results in microglial activation via NOX2, NOX4, and ROS.

The treatments of HMC3 cells with BSA, HIV-1 Tat B, and LPS did not lead to any significant changes in the expression of miR-17 levels. Thus, HIV-1 Tat C specifically activated the microglial cells by targeting NOX2 and NOX4 via miR-17.

This study demonstrated a novel microRNA-mediated mechanism of ROS generation in human microglial cells in response to HIV Tat C protein, which may lead to neuroinflammation and neurodegeneration among HIV-positive patients. This study has been carried out on human microglial cell line (HMC3). Cell lines are based on oncogenic transformations and show drifting patterns of cell surface expression. Therefore, further studies are required on primary cells and/or animal models in light of the current observations of this study.

Acknowledgments and conflict of interest disclosure

References

Babior B. M. (2004) NADPH oxidase. *Curr. Opin. Immunol.* **16**, 42–47.

Baby N., Patnala R., Ling E. A. and ThameemDheen S. (2014) Nanomedicine and its application in treatment of microglia-mediated neuroinflammation. *Curr. Med. Chem.* PMID: 25039775 [Epub ahead of print].

Bartel D. P. (2004) MicroRNAs: genomics, biogenesis, mechanism, and function. *Cell* **116**, 281–297.

Bienert G. P. and Chaumont F. (2014) Aquaporin-facilitated transmembrane diffusion of hydrogen peroxide. *Biochim. Biophys. Acta* **1840**, 1596–1604.

Block M. L. and Hong J. S. (2005) Microglia and inflammation-mediated neurodegeneration: multiple triggers with a common mechanism. *Prog. Neurobiol.* **76**, 77–98.

Boudreau H. E., Emerson S. U., Korzeniowska A., Jendrysik M. A. and Leto T. L. (2009) Hepatitis C virus (HCV) proteins induce NADPH oxidase 4 expression in a transforming growth factor beta-dependent manner: a new contributor to HCV-induced oxidative stress. *J. Virol.* **83**, 12934–12946.

Chang J. R., Mukerjee R., Bagashev A., Del Valle L., Chabrashvili T., Hawkins B. J., He J. J. and Sawaya B. E. (2011) HIV-1 Tat protein promotes neuronal dysfunction through disruption of microRNAs. *J. Biol. Chem.* **286**, 41125–41134.

Chantong B., Kratschmar D. V., Lister A. and Odermatt A. (2014) Dibutyltin promotes oxidative stress and increases inflammatory mediators in BV-2 microglia cells. *Toxicol. Lett.* doi: 10.1016/j.toxlet.2014.03.001. [Epub ahead of print].

Chao C. C., Hu S., Molitor T. W., Shaskan E. G. and Peterson P. K. (1992) Activated microglia mediate neuronal cell injury via a nitric oxide mechanism. *J. Immunol.* **149**, 2736–2741.

Chen P., Mayne M., Power C. and Nath A. (1997) The Tat protein of HIV-1 induces tumor necrosis factor-alpha production. Implications for HIV-1-associated neurological diseases. *J. Biol. Chem.* **272**, 22385–22388.

Clark G. L. and Vinters H. V. (1987) Dementia and ataxia in a patient with AIDS. *West. J. Med.* **146**, 68–72.

Dohgu S., Fleegal-DeMotta M. A. and Banks W. A. (2011) Lipopolysaccharide-enhanced transcellular transport of HIV-1 across the blood-brain barrier is mediated by luminal microvessel IL-6 and GM-CSF. *J. Neuroinflammation* **8**, 167.

Eletto D., Russo G., Passiatore G., Del Valle L., Giordano A., Khalili K., Gualco E. and Peruzzi F. (2008) Inhibition of SNAP25 expression by HIV-1 Tat involves the activity of mir-128a. *J. Cell. Physiol.* **216**, 764–770.

Ensoli B., Barillari G., Salahuddin S. Z., Gallo R. C. and Wong-Staal F. (1990) Tat protein of HIV-1 stimulates growth of cells derived from Kaposi's sarcoma lesions of AIDS patients. *Nature* **345**, 84–86.

Eugenin E. A. and Berman J. W. (2007) Gap junctions mediate human immunodeficiency virus-bystander killing in astrocytes. *J. Neurosci.* **27**, 12844–12850.

Fiore R., Khudayberdiev S., Christensen M., Siegel G., Flavell S. W., Kim T. K., Greenberg M. E. and Schratt G. (2009) Mef2-mediated transcription of the miR379-410 cluster regulates activity-dependent dendritogenesis by fine-tuning Pumilio2 protein levels. *EMBO J.* **28**, 697–710.

Forman H. J. and Torres M. (2001) Redox signaling in macrophages. *Mol. Aspects Med.* **22**, 189–216.

Frank-Cannon T. C., Alto L. T., McAlpine F. E. and Tansey M. G. (2009) Does neuroinflammation fan the flame in neurodegenerative diseases? *Mol. Neurodegener.* **4**, 47.

Frei K., Siepl C., Groscurth P., Bodmer S., Schwerdel C. and Fontana A. (1987) Antigen presentation and tumor cytotoxicity by interferon-gamma-treated microglial cells. *Eur. J. Immunol.* **17**, 1271–1278.

Fu Y., Zhang Y., Wang Z. *et al.* (2010) Regulation of NADPH oxidase activity is associated with miRNA-25-mediated NOX4 expression in experimental diabetic nephropathy. *Am. J. Nephrol.* **32**, 581–589.

Ghosh D., Levault K. R. and Brewer G. J. (2014) Relative importance of redox buffers GSH and NAD(P)H in age-related neurodegeneration and Alzheimer disease-like mouse neurons. *Aging Cell* **13**, 631–640.

Goldstein G. (1996) HIV-1 Tat protein as a potential AIDS vaccine. *Nat. Med.* **2**, 960–964.

Groemping Y. and Rittinger K. (2005) Activation and assembly of the NADPH oxidase: a structural perspective. *Biochem. J.* **386**, 401–416.

Hayes A. M., Qian S., Yu L. and Boris-Lawrie K. (2011) Tat RNA silencing suppressor activity contributes to perturbation of lymphocyte miRNA by HIV-1. *Retrovirology* **8**, 36.

Hazleton J. E., Berman J. W. and Eugenin E. A. (2010) Novel mechanisms of central nervous system damage in HIV infection. *HIV AIDS (Auckl)* **2**, 39–49.

Hu S., Sheng W. S., Schachtele S. J. and Lokensgard J. R. (2011) Reactive oxygen species drive herpes simplex virus (HSV)-1-induced proinflammatory cytokine production by murine microglia. *J. Neuroinflammation* **8**, 123.

Jadhav S. P., Kamath S. P., Choolani M., Lu J. and Dheen S. T. (2014) microRNA-200b modulates microglia-mediated neuroinflammation via the cJun/MAPK pathway. *J. Neurochem.* **130**, 388–401.

Janabi N., Peudenier S., Heron B., Ng K. H. and Tardieu M. (1995) Establishment of human microglial cell lines after transfection of primary cultures of embryonic microglial cells with the SV40 large T antigen. *Neurosci. Lett.* **195**, 105–108.

Jin J., Lam L., Sadic E., Fernandez F., Tan J. and Giunta B. (2012) HIV-1 Tat-induced microglial activation and neuronal damage is inhibited via CD45 modulation: a potential new treatment target for HAND. *Am. J. Transl. Res.* **4**, 302–315.

Jovanovic Z. (2012) Mechanisms of neurodegeneration in Alzheimer's disease. *Med. Pregl.* **65**, 301–307.

Klase Z., Houzet L. and Jeang K. T. (2012) MicroRNAs and HIV-1: complex interactions. *J. Biol. Chem.* **287**, 40884–40890.

Koenig S., Gendelman H. E., Orenstein J. M. *et al.* (1986) Detection of AIDS virus in macrophages in brain tissue from AIDS patients with encephalopathy. *Science* **233**, 1089–1093.

Lavigne M. C., Malech H. L., Holland S. M. and Leto T. L. (2001) Genetic requirement of p47phox for superoxide production by murine microglia. *FASEB J.* **15**, 285–287.

Lee Y., Ahn C., Han J. *et al.* (2003) The nuclear RNase III Drosha initiates microRNA processing. *Nature* **425**, 415–419.

Li B., Bedard K., Sorce S., Hinz B., Dubois-Dauphin M. and Krause K. H. (2009a) NOX4 expression in human microglia leads to constitutive generation of reactive oxygen species and to constitutive IL-6 expression. *J. Innate Immun.* **1**, 570–581.

Li W., Li G., Steiner J. and Nath A. (2009b) Role of Tat protein in HIV neuropathogenesis. *Neurotox. Res.* **16**, 205–220.

Martyn K. D., Frederick L. M., von Loehneysen K., Dinauer M. C. and Knaus U. G. (2006) Functional analysis of Nox4 reveals unique characteristics compared to other NADPH oxidases. *Cell. Signal.* **18**, 69–82.

Mayer V. and Schmidtmayerova H. (1997) Encephalopathy in AIDS–increased formation of beta-chemokines in monocytes after HIV-1 virus infection: mechanisms of CNS involvement. *Bratisl. Lek. Listy* **98**, 330–334.

Mishra R. and Singh S. K. (2013) HIV-1 Tat C modulates expression of miRNA-101 to suppress VE-cadherin in human brain microvascular endothelial cells. *J. Neurosci.* **33**, 5992–6000.

Mishra R., Chhatbar C. and Singh S. K. (2012) HIV-1 Tat C-mediated regulation of tumor necrosis factor receptor-associated factor-3 by microRNA 32 in human microglia. *J. Neuroinflammation* **9**, 131.

Mukerjee R., Chang J. R., Del Valle L. *et al.* (2011) Deregulation of microRNAs by HIV-1 Vpr protein leads to the development of neurocognitive disorders. *J. Biol. Chem.* **286**, 34976–34985.

Panek R. B. and Benveniste E. N. (1995) Class II MHC gene expression in microglia. Regulation by the cytokines IFN-gamma, TNF-alpha, and TGF-beta. *J. Immunol.* **154**, 2846–2854.

Poggi A., Carosio R., Fenoglio D. *et al.* (2004) Migration of V delta 1 and V delta 2 T cells in response to CXCR3 and CXCR4 ligands in healthy donors and HIV-1-infected patients: competition by HIV-1 Tat. *Blood* **103**, 2205–2213.

Ponomarev E. D., Veremeyko T., Barteneva N., Krichevsky A. M. and Weiner H. L. (2011) MicroRNA-124 promotes microglia quiescence and suppresses EAE by deactivating macrophages via the C/EBP-alpha-PU.1 pathway. *Nat. Med.* **17**, 64–70.

Qin L., Liu Y., Wang T., Wei S. J., Block M. L., Wilson B., Liu B. and Hong J. S. (2004) NADPH oxidase mediates lipopolysaccharide-induced neurotoxicity and proinflammatory gene expression in activated microglia. *J. Biol. Chem.* **279**, 1415–1421.

Qin L., Liu Y., Hong J. S. and Crews F. T. (2013) NADPH oxidase and aging drive microglial activation, oxidative stress, and dopaminergic neurodegeneration following systemic LPS administration. *Glia* **61**, 855–868.

Salmen S. and Berrueta L. (2012) Immune modulators of HIV infection: the role of reactive oxygen species. *J. Clin. Cell. Immunol.* **3**, 121.

Sheng W. S., Hu S., Hegg C. C., Thayer S. A. and Peterson P. K. (2000) Activation of human microglial cells by HIV-1 gp41 and Tat proteins. *Clin. Immunol.* **96**, 243–251.

Singh S. K. (2007) miRNAs: from neurogeneration to neurodegeneration. *Pharmacogenomics* **8**, 971–978.

Sorce S. and Krause K. H. (2009) NOX enzymes in the central nervous system: from signaling to disease. *Antioxid. Redox Signal.* **11**, 2481–2504.

Sun G. and Rossi J. J. (2011) MicroRNAs and their potential involvement in HIV infection. *Trends Pharmacol. Sci.* **32**, 675–681.

Suzumura A., Mezitis S. G., Gonatas N. K. and Silberberg D. H. (1987) MHC antigen expression on bulk isolated macrophage-microglia from newborn mouse brain: induction of Ia antigen expression by gamma-interferon. *J. Neuroimmunol.* **15**, 263–278.

Tambuyzer B. R., Ponsaerts P. and Nouwen E. J. (2009) Microglia: gatekeepers of central nervous system immunology. *J. Leukoc. Biol.* **85**, 352–370.

Thannickal V. J. and Fanburg B. L. (2000) Reactive oxygen species in cell signaling. *Am. J. Physiol. Lung Cell. Mol. Physiol.* **279**, L1005–L1028.

Triboulet R., Mari B., Lin Y. L. *et al.* (2007) Suppression of microRNA-silencing pathway by HIV-1 during virus replication. *Science* **315**, 1579–1582.

Turchan-Cholewo J., Dimayuga F. O., Gupta S., Keller J. N., Knapp P. E., Hauser K. F. and Bruce-Keller A. J. (2009a) Morphine and HIV-Tat increase microglial-free radical production and oxidative stress: possible role in cytokine regulation. *J. Neurochem.* **108**, 202–215.

Turchan-Cholewo J., Dimayuga V. M., Gupta S., Gorospe R. M., Keller J. N. and Bruce-Keller A. J. (2009b) NADPH oxidase drives cytokine and neurotoxin release from microglia and macrophages in response to HIV-Tat. *Antioxid. Redox Signal.* **11**, 193–204.

Vilhardt F., Plastre O., Sawada M., Suzuki K., Wiznerowicz M., Kiyokawa E., Trono D. and Krause K. H. (2002) The HIV-1 Nef protein and phagocyte NADPH oxidase activation. *J. Biol. Chem.* **277**, 42136–42143.

Walker D. G., Kim S. U. and McGeer P. L. (1995) Complement and cytokine gene expression in cultured microglial derived from postmortem human brains. *J. Neurosci. Res.* **40**, 478–493.

Westendorp M. O., Frank R., Ochsenbauer C., Stricker K., Dhein J., Walczak H., Debatin K. M. and Krammer P. H. (1995) Sensitization of T cells to CD95-mediated apoptosis by HIV-1 Tat and gp120. *Nature* **375**, 497–500.

Williams K., Bar-Or A., Ulvestad E., Olivier A., Antel J. P. and Yong V. W. (1992) Biology of adult human microglia in culture: comparisons with peripheral blood monocytes and astrocytes. *J. Neuropathol. Exp. Neurol.* **51**, 538–549.

Williams R., Yao H., Peng F., Yang Y., Bethel-Brown C. and Buch S. (2010) Cooperative induction of CXCL10 involves NADPH oxidase: implications for HIV dementia. *Glia* **58**, 611–621.

Xiao H., Neuveut C., Tiffany H. L., Benkirane M., Rich E. A., Murphy P. M. and Jeang K. T. (2000) Selective CXCR4 antagonism by Tat: implications for in vivo expansion of coreceptor use by HIV-1. *Proc. Natl Acad. Sci. USA* **97**, 11466–11471.

Xing S., Shen D., Chen C., Wang J. and Yu Z. (2014) Early induction of oxidative stress in a mouse model of Alzheimer's disease with heme oxygenase activity. *Mol. Med. Rep.* **10**, 599–604.

Yang C. S., Lee H. M., Lee J. Y. *et al.* (2007) Reactive oxygen species and p47phox activation are essential for the Mycobacterium tuberculosis-induced pro-inflammatory response in murine microglia. *J. Neuroinflammation* **4**, 27.

Yao H., Ma R., Yang L. *et al.* (2014) MiR-9 promotes microglial activation by targeting MCPIP1. *Nat. Commun.* **5**, 4386.

Yeung M. L., Bennasser Y., Myers T. G., Jiang G., Benkirane M. and Jeang K. T. (2005) Changes in microRNA expression profiles in HIV-1-transfected human cells. *Retrovirology* **2**, 81.

Zhang L., Dong L. Y., Li Y. J., Hong Z. and Wei W. S. (2012) miR-21 represses FasL in microglia and protects against microglia-mediated neuronal cell death following hypoxia/ischemia. *Glia* **60**, 1888–1895.